TOXICOLOGIC PATHOLOGY ISSN:0192-6233

Volume 18, Number 3, 1990
Printed in U.S.A.

Myopathic Alterations in Extraocular Muscle of Rats Subchronically Fed Pyridostigmine Bromide*[1,2]

STEVEN T. SCHUSCHEREBA, PHILLIP D. BOWMAN, JOSEPH A. VARGAS, THOMAS W. JOHNSON, FRANK J. WOO, AND LUANN MCKINNEY

Letterman Army Institute of Research, Presidio of San Francisco, California 94129-6800

ABSTRACT

To determine if alterations in extraocular muscle morphology occur after subchronic oral administration of pyridostigmine bromide, rats were continuously fed 90 mg/kg in meal and examined at 1, 2, 4, 7, and 15 days. Within the first day, blood acetylcholinesterase activity was reduced by 87% and remained inhibited by 74–91% during the study. Light microscopy demonstrated that by day 1 approximately 3% of the extraocular myofibers were shrunken and invaded by inflammatory cells. The most severe degenerative changes consisting of vacuoles and inflammatory cell infiltration occurred at day 1 with progressively less severe changes at days 2 and 4. At days 7 and 15, 1.3–4.5% of the myofibers still exhibited damage. Ultrastructurally, all presynaptic areas were normal but the postsynaptic areas of affected myofibers at days 1, 2, and 4 showed myofilament and Z-band dissolution, mitochondrial inclusions, subneural fold and T-tubule/sarcoplasmic reticulum vacuolization and subneural fold depth reduction. By days 7 and 15, these changes were diminished in some cases and in others alterations appeared similar to day 1. We conclude that subchronic feeding of pyridostigmine bromide induces myopathic rather than neurogenic changes in rat extraocular muscle and that the myopathy is different in these muscles than in the diaphragm from the same rats.

Keywords. Neuromuscular junction; acetylcholinesterase; anticholinesterases; Z-bands; calcium; degeneration; regeneration

INTRODUCTION

The reversible anticholinesterase agent pyridostigmine bromide (PB) is used in the treatment of myasthenia gravis and could be used by U.S. military personnel and their allies as part of a preexposure antidote for nerve poisons that irreversibly inhibit acetylcholinesterase (ACHase) (13). Anticholinesterase drugs also have ophthalmologic applications in inducing miosis and in the treatment of primary and secondary glaucoma (21). Therefore, potential toxic effects must be considered.

Previous studies (7, 8, 17) on acute toxicity of acetylcholinesterase inhibitors have shown rapid inactivation of cholinesterases at the mammalian neuromuscular junction (NMJ). Myofibers respond with spasm, hypercontraction, degeneration, and necrosis. Ultrastructurally, in muscles such as diaphragm, soleus and extensor digitorum longus, the myopathy consists of large diameter vacuoles in the presynaptic zone, dilation of mitochondria, Z-band dissolution, and myofilament contraction and degeneration (7, 17). This damage is thought to be mediated by increased intracellular calcium (14) and has been suggested to be specific for type I fibers (7).

There is a lack of morphologic data concerning the effects of anticholinesterase agents on the faster and more complex extraocular muscles (EOMs). In this study, we report the morphologic effects of subchronic feeding of PB on EOMs. Unlike other skeletal muscle after PB treatment, EOMs show a high percentage of altered NMJs at the electron microscope level. The primary site of alteration in the NMJs is the postsynaptic region, although the whole myofiber can eventually be involved.

METHODS

Eighteen male Sprague-Dawley rats (Simonsen, Gilroy, CA) weighing 180–250 g each were used in

* Address correspondence to: Commander, Letterman Army Institute of Research, SGRD-ULY-OH ATTN: S. T. Schuschereba, Presidio of San Francisco, California 94129-6800.

[1] The opinions and assertions contained herein are the private views of the authors and are not to be construed as official nor do they reflect the views of the Department of the Army or the Department of Defense (AR 360-5).

[2] The studies described in this report were reviewed and approved by the Institutional Review Committee/Animal Care and Use Committee at Letterman Army Institute of Research. The manuscript underwent Institutional peer review prior to submission for publication. In conducting the research described herein, the investigators adhered to the "Guide for the Care and Use of Laboratory Animals," DHEW Publication (NIH) 85-23.

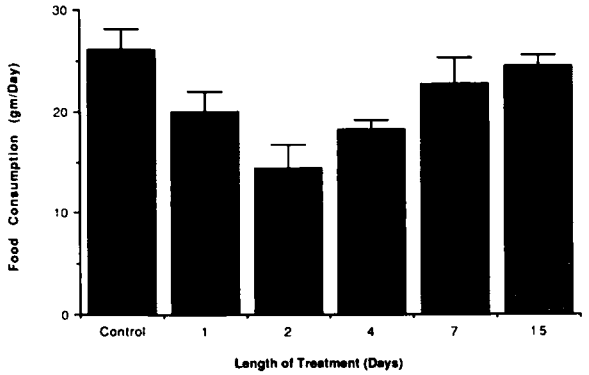

FIG. 1.—Food consumption for each animal group during constant PB (90 mg/kg/day) dosing for days 1, 2, 4, 7, and 15. Error bars represent the SEM ($p = 0.10$).

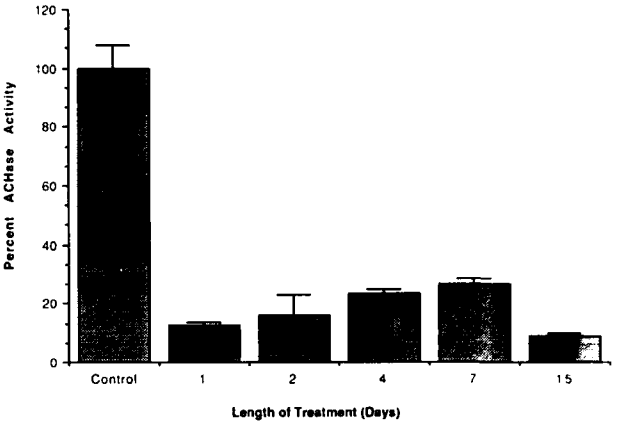

FIG. 2.—Blood acetylcholinesterase activity after constant PB (90 mg/kg/day) dosing for days 1, 2, 4, 7, and 15. Error bars represent the SEM ($p \leq 0.001$).

this study. Beginning at time zero, 15 rats were fed meal containing an amount of pyridostigmine bromide (Hoffman-La Roche, Nutley, NJ, Lot #590034) calculated to provide a dose of 90 mg/kg/day (4). This amount was determined by recording the daily food consumption during the preceding week and adding sufficient pyridostigmine bromide to provide 90 mg/kg/day. Adjustments for variation in food intake were made weekly and a new amount of drug added accordingly. At each time point (days 0, 1, 2, 4, 7, and 15), the 3 animals to be euthanized were bled from the tail vein (using a 22 gauge needle wetted with heparin) to determine acetylcholinesterase levels. At day 0, control animals did not receive PB. Acetylcholinesterase measurements were made within 2–5 min after collection using the method of Siakotos et al (20). Acetylcholinesterase activity was determined by measuring the rate of [1-^{14}C] acetyl-β-methylcholine hydrolysis. Incubation of substrate with whole blood samples was carried out in phosphate buffer for 5 min at 37°C. [1-^{14}C] acetic acid was quantitated by scintillation counting.

To eliminate side effects of anesthesia, rats were decapitated. Eyes were enucleated with attached muscles, hemisected and fixed within 5 min of death in cacodylate-buffered 2.5% glutaraldehyde and 2.0% paraformaldehyde solution at 4°C pH 7.4 (11). After postfixation in osmium tetroxide for 1 hr, dehydration in a graded series of ethanols, and transitioning in propylene oxide, one eye from each rat was embedded in Spurr's plastic resin (Polysciences Inc., Warrington, PA). One-micron thick plastic sections of muscle were stained with methylene blue (9) and examined for the presence of small nerve bundles next to the myofibers. The presence of small nerve bundles in an area of interest provided a greater possibility of finding NMJs at the electron microscope level, so these areas were isolated for further analysis. Thin sections were cut with a diamond knife, stained with uranyl acetate and lead citrate in an LKB Ultrostainer (LKB Instruments, Inc., Gaithersburg, MD) and then examined and photographed with a Zeiss EM-10CA transmission electron microscope at 60 kV.

The extent of myofiber damage was determined at light microscopy by quantitating the number of damaged myofibers as a fraction of the total number of myofibers in a section. One section from the last 3 taken from a given block was randomly selected for quantitation. The criterion for light microscopic myofiber damage was the presence of infiltrated inflammatory cells, dark-stained or mottled myofilaments, vacuoles, and edema. Shrunken and crenated myofibers at the later time points were difficult to quantitate by light microscopy.

For transmission electron microscopy, 5–9 different NMJ sites were located and photographed in each of 3 eyes at all 6 time points. No attempt was made to identify specific extraocular muscles, fiber types or the type of innervation. Damaged NMJs were counted from electron micrographs to determine the fraction of the total NMJs damaged. The criterion for electron microscopic NMJ damage was the presence of any ultrastructural alteration that was not present in control tissue.

When appropriate, a one-way analysis of variance model was used to analyze the data. If a significant F-value occurred, the Newman-Keuls method of multiple comparisons was used to determine which means differed. All statistical tests were performed at the 0.05 level of significance.

RESULTS

No remarkable clinical signs were noted except that treated animals were somewhat more lethargic than untreated animals. Food consumption by the rats initially dropped and then returned to near nor-

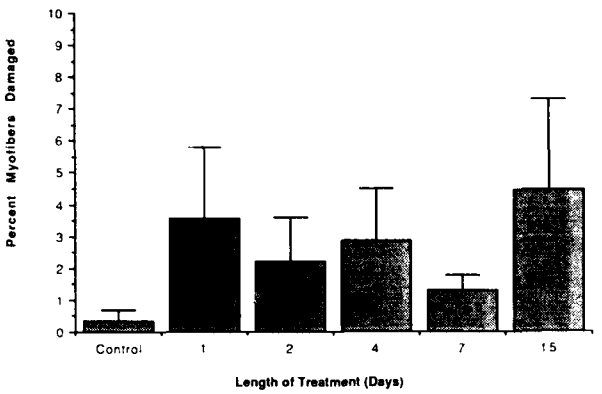

FIG. 3.—Frequency of myofiber damage after constant PB (90 mg/kg/day) dosing for days 1, 2, 4, 7, and 15. Error bars represent the SEM.

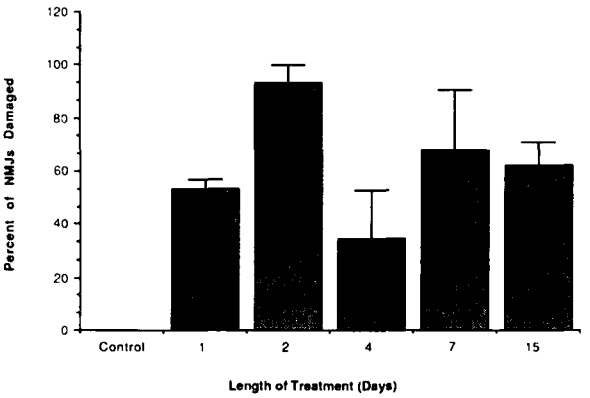

FIG. 4.—The percent of damaged neuromuscular junctions after constant PB (90 mg/kg/day) dosing for days 1, 2, 4, 7, and 15. Error bars represent the SEM ($p = 0.004$).

mal levels (Fig. 1). Pyridostigmine bromide administration inhibited blood acetylcholinesterase activity 74–91% compared to control values for the 15 day duration of the study. A significant difference was found between the control and all of the PB treated groups (Fig. 2).

Determination of the number of damaged myofibers by light microscopy in 1-micron plastic sections, as a percent of total myofibers, showed that, during the course of the experiment, 1.3–4.5% of the myofibers in PB fed rats contained phagocytic inflammatory cells, myofilament degeneration, ede-

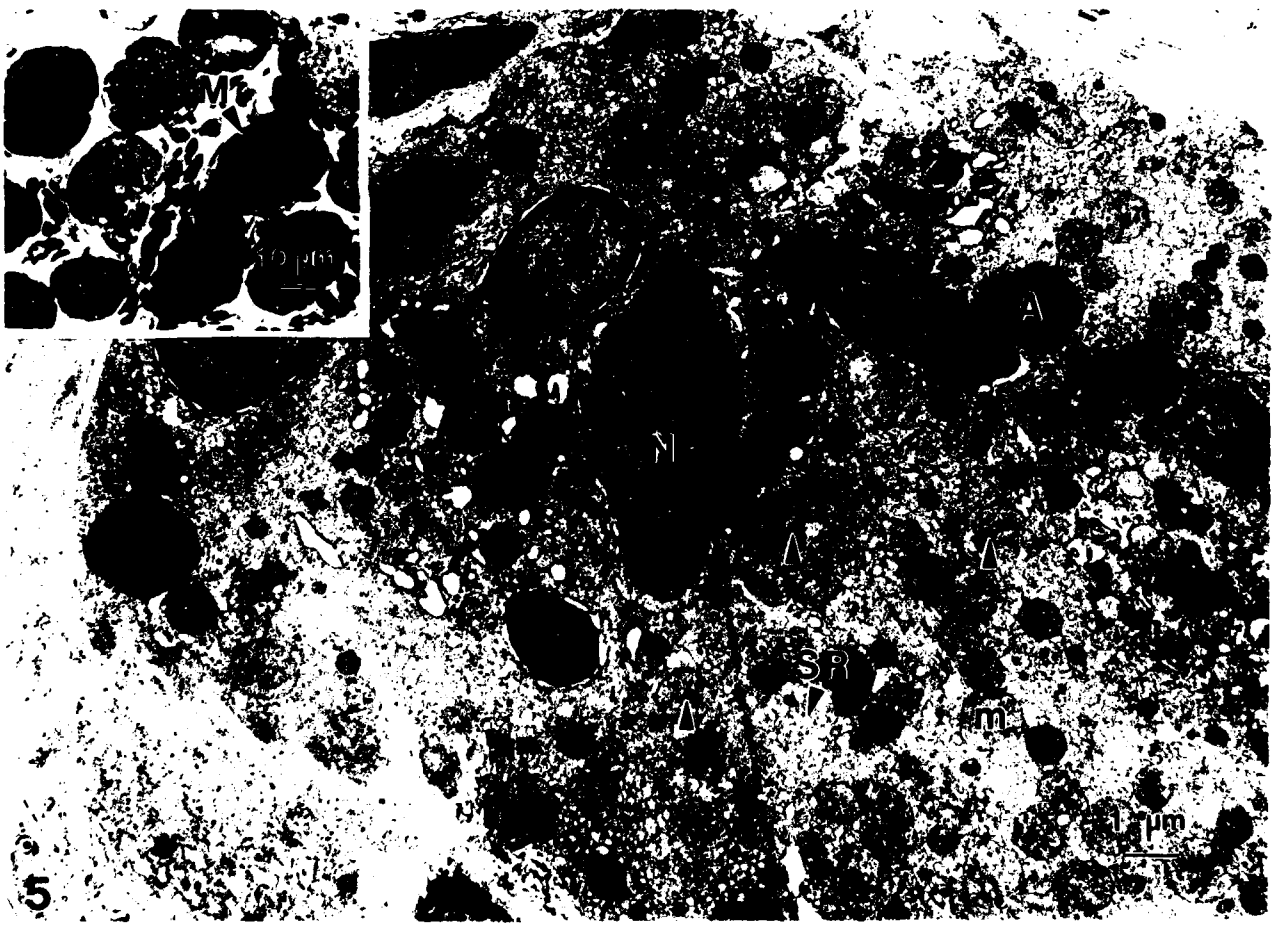

FIG. 5.—Transmission electron micrograph (TEM) of EOM at day 1 of rat fed PB. Abnormal changes include nuclei (N) of inflammatory cells in the myofiber, dilated sarcoplasmic reticulum (SR), disrupted myofilaments, phagosomes with large mitochondrial aggregates (A), and inclusions (arrows) in swollen mitochondria (m). Bar = 1.0 μm. Inset: Light micrograph of the same myofiber (M). Bar = 10.0 μm.

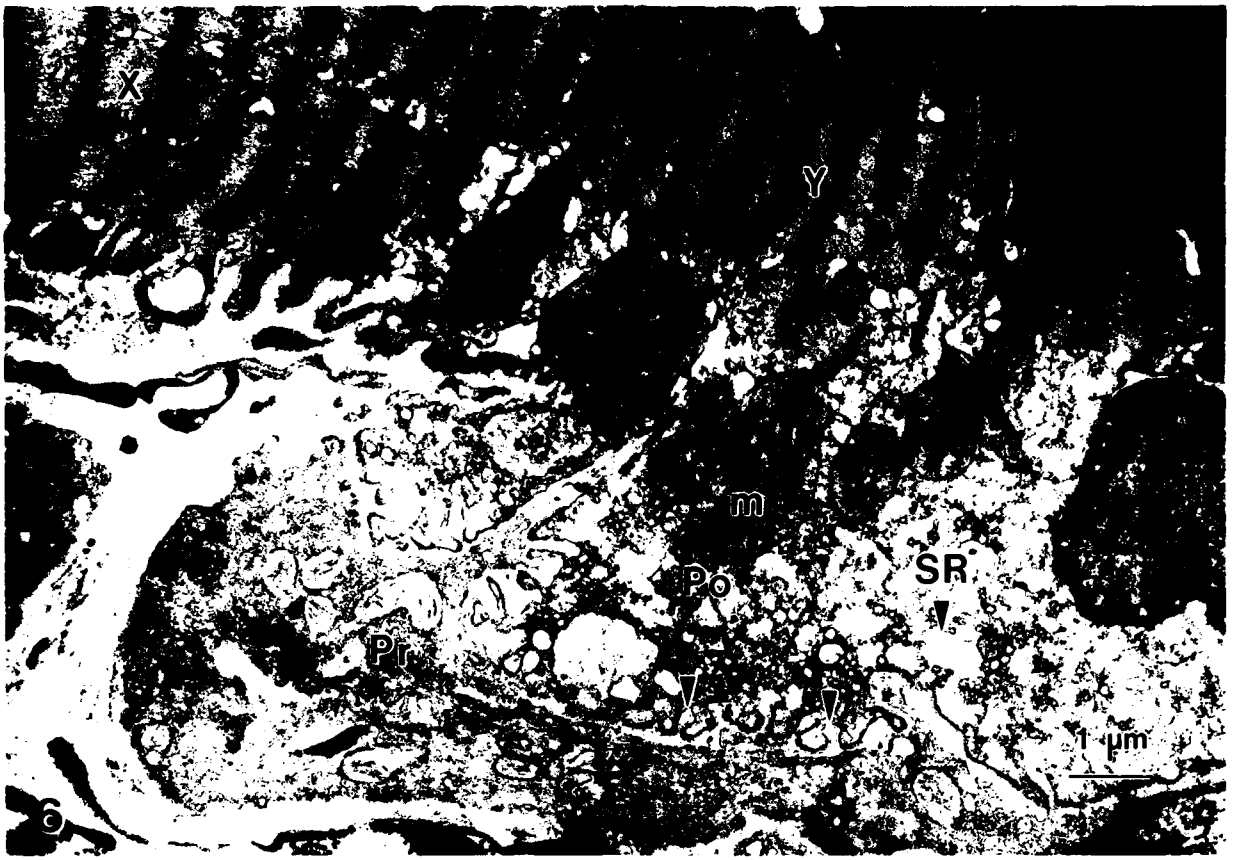

FIG. 6.—TEM of EOM at day 1 of rat fed PB. The presynaptic (Pr) area of the NMJ is relatively normal. The postsynaptic (Po) area, however, contains swollen sarcoplasmic reticulum (SR) and mitochondria (m), and a diminution of subneural fold depth (arrows). Hypercontraction of the Z-bands is present directly opposite the presynaptic area at Y (compare Z-band spacing with area at X). Bar = 1.0 µm.

ma, or vacuolization (Fig. 3). EOMs from controls showed only slight myofiber damage without inflammatory cell infiltration. This baseline damage was confined to a few peripheral myofibers and is believed due to artifact produced during enucleation of the eye.

Quantitation of damaged NMJs by transmission electron microscopy, however, demonstrated that a large number were affected by the treatment (Fig. 4). Analysis of the data indicated that a statistically significant difference was present between the experimental and control groups. NMJs from all control animals had normal pre- and postsynapses.

Ultrastructurally, by the end of the first day of treatment, severely affected myofibers contained macrophages, dilated sarcoplasmic reticulum, disrupted myofilaments, and swollen mitochondria with dense inclusions (Fig. 5). All mitochondria from control myofibers that we observed were normal and did not contain inclusions. Light microscopy revealed that damaged myofibers were invaded by phagocytic inflammatory cells (Fig. 5, inset). Alterations of the NMJ were confined to the postsynaptic area (Fig. 6). A comparison of Z-band spacing measurements on day 1 of PB treatment indicated that spacing of Z-bands opposite the nerve terminal was about 50% of the control value (Fig. 6).

By the end of day 2 of PB treatment, the postsynaptic area of the NMJs showed additional alterations that included the subneural folds and synaptic cleft (Figs. 7A and 7B). In some animals, the postsynaptic regions of all NMJs examined were affected while the presynaptic areas of the NMJ were not.

By day 4 of PB treatment, severe changes were observed in the synaptic cleft (Fig. 7C). The postsynaptic zones showed disrupted Z-bands directly opposite the nerve terminal (Fig. 8A). In addition, more advanced degenerative changes in the Z-bands included condensed areas of sarcoplasm opposite the nerve terminal (Fig. 8B). Other myofibers contained extensive sarcoplasmic reticulum vacuolization and myofilament degeneration without condensed sarcoplasm (Fig. 8C). In these examples, the subneural folds were intact.

By day 7 of PB treatment, focal myofiber necrosis (Fig. 8D) and ultrastructural alterations (intensive inflammatory cell invasion), similar to the earlier time points, were seen. Occasionally, leptomeres

(cross-striated bundles of filaments between the Z-bands) thought to be indicative of degenerative change (15), were found (Fig. 8D, inset).

By day 15 of PB treatment, all of the above mentioned changes were evident, except in some instances changes were not as severe as in earlier time points. However, small, degenerated myofibers were present and other myofibers contained large vacuoles with autophagosomal material. Compared to earlier observations, some of the NMJs showed mild synaptic cleft changes (Fig. 9A) while others had wider and more distorted synaptic clefts filled with large quantities of vesicular debris (Fig. 9B), and in some cases cell processes (Fig. 9C, inset). Some myofiber nuclei indicated a regenerative response, evidenced by the presence of large nucleoli, an abundance of light-stained euchromatin (the active and functional form of chromatin involved in transcription), and margination of the heterochromatin adjacent to advanced degenerating nuclei (Figs. 9C and 9D). In other myofibers, the presence of myelin forms and normal sarcoplasmic reticulum provided evidence of autophagocytosis and regeneration, respectively (Fig. 9E).

Discussion

In a previous study (3), we have shown that including PB in feed causes a prolonged and sustained depression of blood acetylcholinesterase activity and distinct morphologic alterations in diaphragm muscle or rats. The EOMs, with the exception of the levator palpebrae superioris and the retractor bulbi, differ from other skeletal muscles as they are more complex in their fiber composition (6 vs 3 fiber types) and they are either singly or multiply innervated (16). They are also the fastest twitch fibers on record with tetanic fusion frequencies about 10 times faster (350–450 Hz) than those of the diaphragm muscle (25–30 Hz) (2, 19). Pyridostigmine bromide, however, is thought primarily to affect slow twitch myofibers (7). Since it was not feasible to separate fiber types in this study without enzymatic staining and extensive morphologic characterization (16), we did not attempt to do so.

After PB treatment, light microscopy revealed that 1.3–4.5% of the myofibers were affected and transmission electron microscopy showed changes in 35–93% of the randomly observed NMJs. Ultrastructurally, the myopathy was confined to the postsynaptic region of the NMJs. In addition, widening of the synaptic cleft and the presence of vesicles in the cleft were common features. This last feature has been reported in human myasthenia gravis in the absence of anticholinesterase treatment (5). In myasthenia gravis, the tips of the subneural folds, which are rich in acetylcholine receptors, are thought to

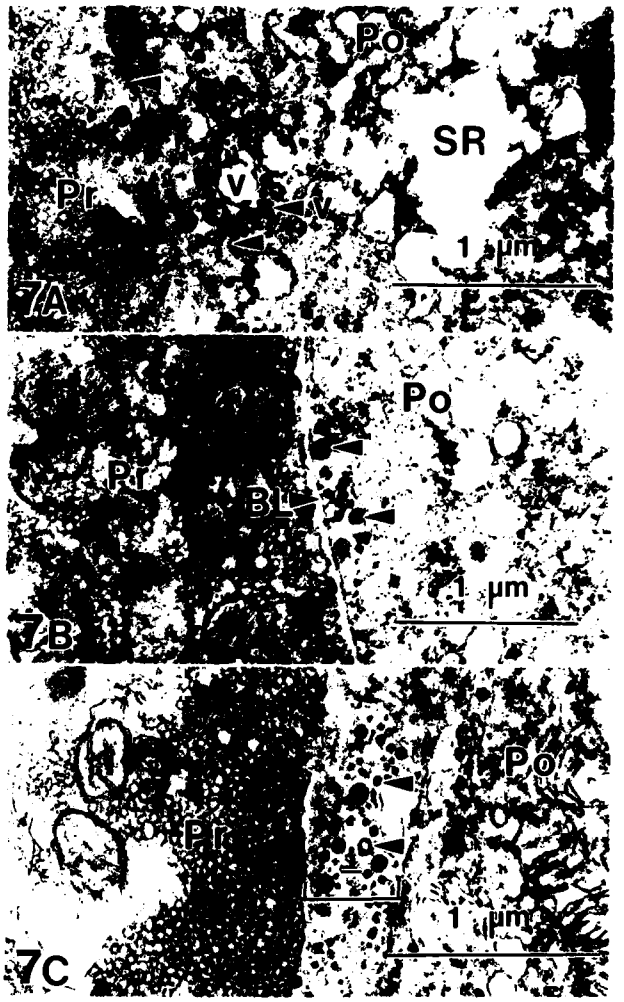

FIG. 7.—TEMs of synaptic cleft changes in EOM of rat fed PB. Bars = 1.0 μm. A. Day 2. The presynaptic (Pr) area of the NMJ appears relatively normal. The postsynaptic (Po) area, however, contains vacuolated sarcoplasmic reticulum (SR) and a zone of small and large vesicles (v) with dense inclusions near the synaptic cleft. Subneural folds are absent (arrows). B. Day 2. Small dense vesicles (arrows) are on the postsynaptic side of the basal lamina (BL) of the synaptic cleft. C. Day 4. The presynapse (Pr) is normal. The synaptic cleft (bracket) has a wider than normal gap (bar in cleft = normal gap width) and is filled with light and dense vesicles (arrows).

degenerate; and degraded remnants of these folds remain in widened synaptic clefts (5). In addition, our results suggest but do not confirm that the cleft vesicles may also originate from the extrusion of what may be excess calcium at the NMJ (Fig. 7).

Recent studies have indicated that PB administration produced both neurogenic and myopathic changes at the NMJ of diaphragm and soleus muscles (8). The changes we observed are consistent with a myopathy observed by others (1, 6, 12, 17) after experimental poisoning with anticholinesterase agents such as carbamates and nerve agent organo-

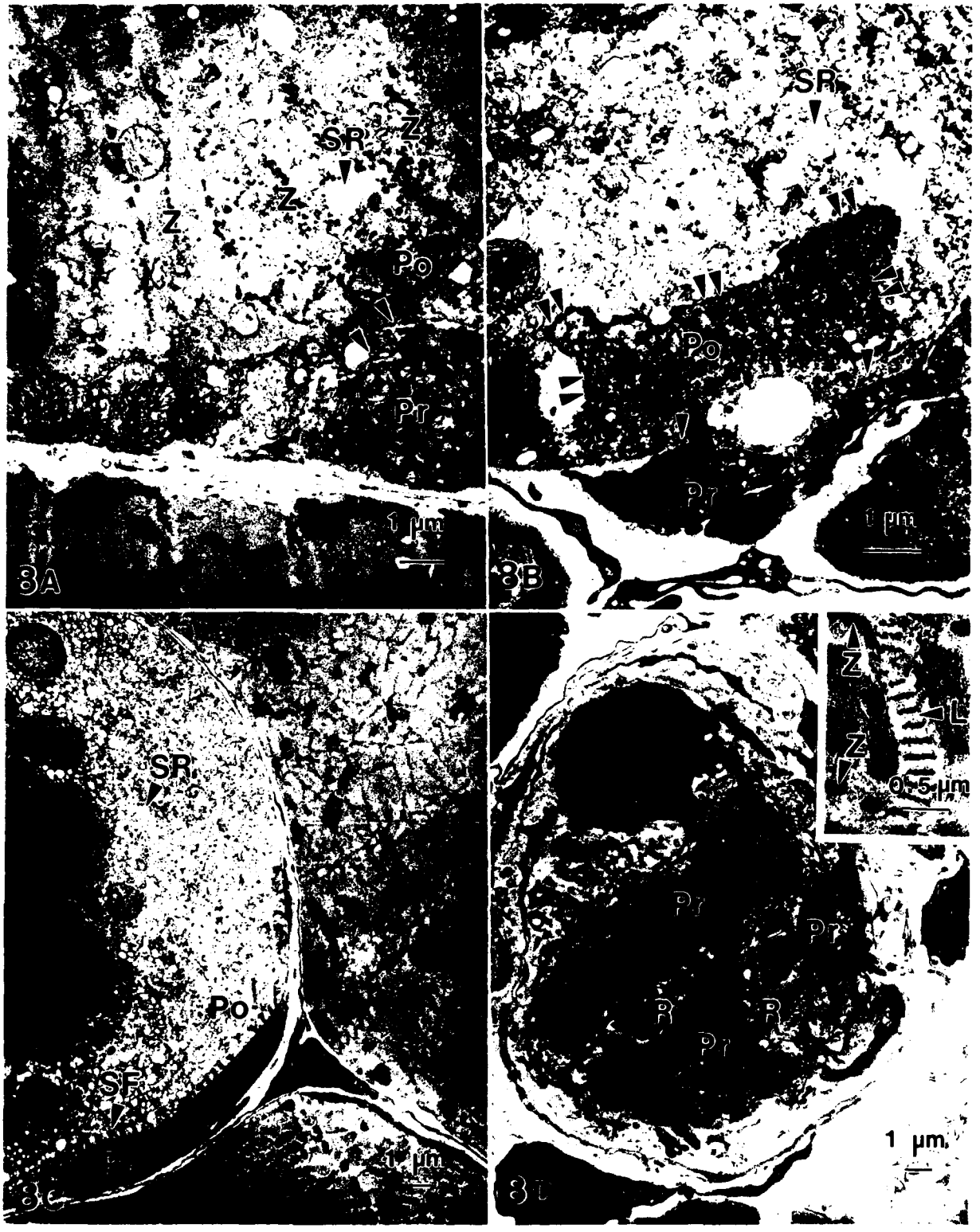

FIG. 8.—TEMs of EOMs of rats fed PB. Bars = 0.5 or 1.0 µm. A. Day 4. The presynaptic (Pr) area is normal, but the postsynaptic (Po) zone contains vacuolated sarcoplasmic reticulum (SR), loss of subneural folds (arrows), and disruption of the Z-bands (Z) directly opposite the nerve terminal (compare with Fig. 5). B. Day 4. Similar changes are present in this myofiber, except that condensed cytoplasm (double arrows) is present directly opposite the nerve (compare with Figs. 5 and 7). C. Day 4. The presynaptic (Pr) area is normal, but the postsynaptic (Po) zone contains a highly vacuolated sarcoplasmic reticulum (SR). The subneural folds (SF) are intact. D. Day 7. Remnants (R) of a degenerative myofiber are surrounded by the presynaptic (Pr) nerve terminals. Inset: Leptomere (L) is present between Z-bands (Z).

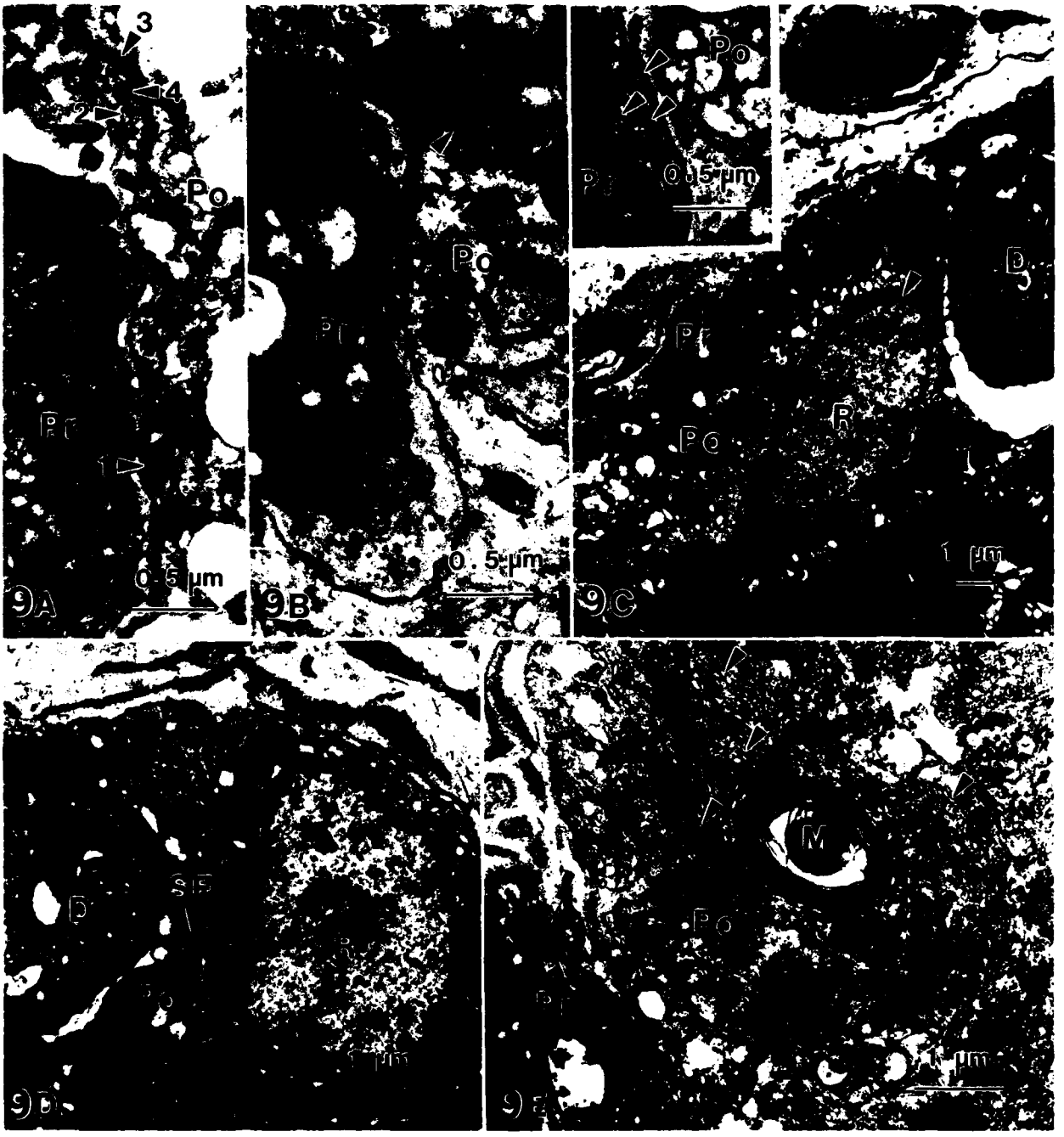

FIG. 9.—TEMs of EOM at day 15 of rat fed PB. Presynapses (Pr) and postsynapses (Po). Bars = 0.5 or 1.0 µm. A. Vesicles bleb from the postsynaptic membrane (arrow #1). Other vesicles bleb from the basal lamina of the cleft (arrow #2). The postsynaptic membrane contains dense zones (arrow #3) that may form the dense vesicles in the cleft (arrow #4). B. The synaptic cleft is highly distorted. A portion of the presynapse (arrow) is infolded next to the subneural folds. C. A degenerating nucleus (D) is present adjacent to a marginated (arrow) and lightly stained nucleus (R) indicating a regenerative response by the myofiber. Presynapse (Pr). Inset: A synaptic cleft contains cytoplasmic processes (arrows). D. Subneural folds (SF) separate a degenerating nucleus (D) from a regenerating nucleus (R). E. Large myelin (M) forms similar to the ones found in regenerating diaphragm muscle are present in the postsynaptic area. Normal sarcoplasmic reticulum (arrows) is present adjacent to the myelin form.

phosphates. The myopathy described in these previous studies could be attributed to severe and prolonged endplate depolarization, presumably caused by high local concentrations of unhydrolyzed acetylcholine which produce elevated intracellular levels of calcium in the myofiber (10, 14, 18). The presence of inclusions, presumably containing calcium, in mitochondria and sarcoplasmic reticulum,

at days 1 and 2 after PB treatment provides evidence for a similar mechanism responsible for the myopathy in the present study. In addition, focal hypercontraction of the Z-bands and their subsequent deterioration opposite the nerve terminal lend further support to a pathogenetic role for increased levels of calcium. Perhaps the widening of the cleft, the decrease in the subneural fold surface area, and the potential extrusion of what may be excess calcium is the mechanism by which end-plates accommodate prolonged acetylcholinesterase inhibition. Conversely, perhaps an injured myofiber, because of hypercontraction, cannot maintain cell surface moieties to preserve normal junction apposition.

The reason why only a portion of the myofibers are severely affected is not known, but may be related to fiber type, function or both. It is also not understood why, at the ultrastructural level, the NMJ has such frequent and widespread alteration. In a previous study of diaphragm muscle, evidence of degeneration decreased from day 1 to day 15 with no evidence of degeneration present by day 15 (3). In our study, evidence of both degeneration and regeneration was found by day 15 of PB treatment. When the degenerative changes from the diaphragm (3) are compared to that of the EOMs from the same rats, the EOMs suggest a greater sensitivity to PB, as severe morphologic alterations are still present by day 15 of PB dosing. Furthermore, if we can assume that damaged myofibers are removed at the same rate from both EOMs and diaphragm, then our results suggest that new sets of myofibers are altered as PB dosing is continued. This contention is supported by morphological changes at day 7 and day 15 that are similar to those occurring on day 1.

In summary, subchronic administration of PB in feed produces myopathic changes at the light microscopic level in 1.3–4.5% of the myofibers in the rat EOM. By transmission electron microscopy, 35–93% of only the postsynaptic portions of the NMJs are affected, indicating that EOMs are more sensitive to the effects of PB than diaphragm and soleus muscles. Hypercontraction, dissolution of Z-bands, and mitochondrial inclusions suggest that increased intracellular calcium is the most likely cause of damage. Widening of the synaptic clefts, the presence of cleft vesicles, and evidence of muscle regeneration may suggest some mechanism(s) of adapation to PB. Finally, the difference in morphologic alteration, specifically at the later time points, in the myofibers of the diaphragm and EOMs has two possible explanations: either the removal of myofibers differs between the diaphragm and the EOMs or the myofibers of EOMs continue to be altered when those of the diaphragm have adapted.

ACKNOWLEDGMENTS

We would like to thank Virginia Gildengorn for assistance with statistical analysis and Susan Siefert for editorial comments. Portions of this work were presented at the meeting of the Association for Research in Vision and Ophthalmology in Sarasota, FL, May 1988.

REFERENCES

1. Ariens AT, Meeter E, Wolthius OL, and Van Benthem RMJ (1969). Reversible necrosis at the end-plate region in striated muscles of the rat poisoned with colinesterase inhibitors. *Experientia* 25: 57–59.
2. Bach Y, Rita P, and Ito F (1966). *In vivo* studies on fast and slow muscle fibers in cat extraocular muscles. *J. Gen. Physiol.* 49: 1177–1198.
3. Bowman PD, Schuschereba ST, Johnson TW, Woo FJ, McKinney L, Wheeler CR, Frost DF, and Korte DW (1989). Myopathic changes in diaphragm of rats fed pyridostigmine bromide subchronically. *Fundam. Appl. Toxicol.* 13: 110–117.
4. Chan PK, O'Hara GP, and Hayes AW (1982). Principals and methods for acute and subchronic toxicity. In: *Principals and Methods of Toxicology*, AW Hayes (ed). Raven Press, New York, pp. 1–51.
5. Engel AG, Tsujihata MT, Lindstrom JM, and Lennon VA (1976). The motor end plate in myasthenia gravis and in experimental autoimmune myasthenia gravis. A quantitative ultrastructural study. *Annals of N.Y. Acad. of Sciences.* Myasthenia gravis. 274: 60–78.
6. Fenichel GM, Kibler WB, Olson WH, and Dettbarn WD (1972). Chronic inhibition of cholinesterase as a cause of myopathy. *Neurology* 22: 1026–1033.
7. Gebbers J-O, Lotscher M, Kobel W, Portmann R, and Laissue J-A (1986). Acute toxicity of pyridostigmine in rats: Histological findings. *Arch. Toxicol.* 58: 271–275.
8. Hudson CS, Foster RE, and Kahng MW (1986). Neuromuscular toxicity of pyridostigmine bromide in the diaphragm, extensor digitorum longus and soleus muscles of the rat. *Fundam. Appl. Toxicol.* 5: S260–S269.
9. Humphrey CD and Pittman FE (1974). A simple methylene blue-azure-II basic fuchsin stain for epoxy-embedded tissue sections. *Stain Technol.* 49: 9–14.
10. Jackson MJ, Jones DA, and Edwards HT (1984). Experimental skeletal muscle damage: The nature of the calcium-activated degenerative processes. *Eur. J. Clin. Invest.* 14: 369–374.
11. Karnovsky MJ (1965). A formaldehyde-glutaraldehyde fixative of high osmolality for use in electron microscopy. *J. Cell Biol.* 27: 137A–138A.
12. Kawabuchi M, Osame M, Watanabe S, Igata A, and Kanaseki R (1976). Myopathic changes at the end-plate induced by neostigmine methylsulfate. *Experientia* 32: 623–625.
13. Leadbeater L, Inns RH, and Rylands JM (1985).

Treatment for poisoning by Soman. *Fundam. Appl. Toxicol.* 5: S225–S231.

14. Leonard JP and Salpeter MM (1979). Agonist-induced myopathy at the neuromuscular junction is mediated by calcium. *J. Cell Biol.* 82: 811–819.
15. Mastaglia FL and Hudgson P (1981). Ultrastructural studies of diseased muscle. In: *Disorders of Voluntary Muscle*, 4th ed., J Walton (ed). Churchill Livingstone, New York, pp. 296–356.
16. Mayr R (1971). Structure and distribution of fibre types in the external eye muscles of the rat. *Tissue Cell.* 3: 433–462.
17. Meshul CK, Boyne AF, Deshpande SS, and Albuquerque EX (1985). Comparison of the ultrastructural myopathy induced by anticholinesterase agents at the end plates of rat soleus and extensor muscles. *Exp. Neurol.* 89: 96–114.
18. Salpeter MM, Leonard JP, and Kasprzak H (1982). Agonist-induced postsynaptic myopathy. *Neurosci. Comment.* 1: 73–83.
19. Salpeter MM, Rodgers AW, Kasprzak H, and McHenry FA (1978). Acetylcholinesterase in the fast extraocular muscle of the mouse by light and electron microscope autoradiography. *J. Cell Biol* 78: 274–285.
20. Siakotos AN, Filbert M, and Hester R (1969). A specific radioisotopic assay for acetylcholinesterase and pseudocholinesterase in brain and plasma. *Biochem. Med.* 3: 1–12.
21. Taylor P (1985). Anticholinesterase agents. In: *The Pharmacological Basis of Therapeutics*, 7th ed., AG Gilman, LS Goodman, TW Rall, and F Murad (eds). Macmillan Pub. Co., New York, p. 123.